

# The Impact of Fiber Length on the Gain and Efficiency of Erbium Doped Amplifier

Naquiuddin Razali<sup>1</sup>, Noor Azura Awang<sup>1\*</sup>

<sup>1</sup> Department of Physics and Chemistry, Faculty of Applied Sciences and Technology, UTHM Kampus Cawangan Pagoh, Hab Pendidikan Tinggi Pagoh, KM 1, Jalan Panchor, 84600 Pagoh, Muar, Johor, MALAYSIA.

\*Corresponding Author: [norazura@uthm.edu.my](mailto:norazura@uthm.edu.my)

DOI: <https://doi.org/10.30880/ekst.2025.05.01.015>

## Article Info

Received: 31 December 2024

Accepted: 16 January 2025

Available online: 20 July 2025

## Keywords

Erbium-Doped Fiber Amplifiers, Optical Communication, Gain Optimization, Fiber Length, ASE Noise, DWDM

## Abstract

Erbium-doped fibre amplifiers (EDFAs) are critical components of modern optical communication networks, delivering high gain and efficient signal amplification over long distances. This study looks into how fibre length affects the gain and efficiency of EDFAs, with a focus on optimising performance for real-world applications. Using numerical simulations and experimental validations in OptiSystem software, the researchers investigate the impact of systematically increasing fibre length on gain, noise figure, and power conversion efficiency. The findings show a nonlinear relationship: excessively long fibres cause amplified spontaneous emission (ASE) noise and poor efficiency, whereas shorter fibres fail to achieve enough signal amplification. The study finds the best fibre length for balancing gain and efficiency while minimising noise, which will help to develop high-performance EDFAs. These findings provide useful insights for improving optical networks, particularly in applications like Dense Wavelength Division Multiplexing (DWDM), and emphasise the necessity of rigorous parameter optimisation in the advancement of optical communication technology.

## 1. Introduction

Optical communication techniques transformed current information technology by allowing high-speed data transmission over large distances with minimum signal loss. Erbium-doped fibre amplifiers (EDFAs) are critical components of these systems because they enhance weak optical signals without requiring electrical conversion. EDFAs are especially useful because of their high gain, wide bandwidth, and compatibility with Dense Wavelength Division Multiplexing (DWDM), a critical technology for enhancing optical network capacity and efficiency. These amplifiers have become indispensable for providing consistent, high-capacity data transmission in applications such as telecommunications, cloud computing, and global internet infrastructure [1] and [2].

Fibre length, erbium doping concentration, and pump power are some of the variables that affect EDFA performance. Because it directly influences the interaction between erbium ions and the optical signal, which determines the amplifier's gain, efficiency, and noise figure, fibre length is particularly important. While very lengthy fibres diminish efficiency and introduce amplified spontaneous emission (ASE) noise, shorter fibres lead to insufficient signal amplification [3] and [4]. For EDFAs to function well in high-speed and long-distance communication systems, an ideal equilibrium between these variables must be struck [5].

Optimising EDFA performance is difficult, though, especially in DWDM systems where several wavelength channels need to be amplified at once. The design procedure is made more difficult by the nonlinear relationship between fibre length, gain, and efficiency. According to [6] and [7], for example, while increasing fibre length initially improves gain, it eventually results in decreased efficiency and increased noise due to ASE and pump

power depletion. Addressing the growing need for high-speed, long-distance communication and enhancing the overall effectiveness of EDFAs require an understanding of the trade-offs between these characteristics [8].

Through numerical calculations and experimental validation using OptiSystem software, this work examines how fibre length affects the gain and efficiency of EDFAs. It determines the ideal fibre length for real-world applications by analysing important factors including gain, noise figure, and power conversion efficiency. By tackling these issues, our study advances the creation of high-performance, energy-efficient EDFAs for submarine networks, DWDM systems, and other cutting-edge optical applications [8] and [9].

Analysing how different fibre lengths affect EDFA gain, looking at how fibre length affects amplifier efficiency, and figuring out the ideal fibre length for best performance are the goals of this study. In order to meet the increasing demand for dependable and scalable optical communication systems worldwide, these discoveries seek to improve EDFA design [11] and [12].

## 2. Methodology

This study examines the performance of erbium-doped fibre amplifiers (EDFAs) using numerical simulations using OptiSystem software. Key components like the pump laser, continuous wave (CW) laser, ideal multiplexer (mux), dual-port Wavelength Division Multiplexer (WDM) analyser, erbium-doped fibre, and optical spectrum analyser (OSA) can all be integrated using OptiSystem, a flexible tool for designing, simulating, and assessing optical communication systems [3] and [10]. These elements are set up to mimic actual circumstances, making it possible to systematically examine the effects of fibre length on efficiency, noise figure, and gain [9] and [11].

The energy source needed to excite the erbium ions in the fibre and enable stimulated emission signal amplification is the pump laser. The power of the pump laser, which operates at wavelengths of 980 nm or 1480 nm, directly affects population inversion in the erbium ions. While too much pump power introduces amplified spontaneous emission (ASE) noise, which lowers efficiency, too little pump power leads to inadequate amplification [4]. Operating at common communication wavelengths in the C-band (1530–1565 nm) or L-band (1570–1610 nm), the CW laser is set up to mimic the input optical signal. Dense Wavelength Division Multiplexing (DWDM) systems' multi-channel data transmission is replicated in this configuration [6] and [8].

In order to provide effective signal integration with low losses, the pump laser and CW laser signals are combined into a single optical route using an ideal multiplexer (mux) [5]. The erbium-doped fibre (EDF), the primary amplification medium, receives the combined signals. The EDF uses stimulated emission to increase the input signal after being doped with erbium ions. Because longer fibres introduce ASE noise and power depletion, meanwhile shorter fibres may result in inadequate amplification, the fibre length is a crucial element in defining the gain and noise characteristics of the amplifier [7] and [9]. This study determines the ideal fibre length for effective signal amplification by methodically altering it and assessing the effect on performance.

The dual-port Optical Spectrum Analyser (OSA) and Wavelength Division Multiplexer (WDM) analysers are used to examine the amplified signal. The WDM analyser provides information about the behaviour of the EDFA in DWDM systems by measuring optical power, gain, and noise characteristics across several wavelength channels [1]. By capturing the noise figure and gain spectrum, the OSA makes it possible to identify nonlinear effects like ASE [3]. When combined, these elements offer a thorough assessment of the EDFA's performance in a range of operational scenarios.

The first step in the research process is to integrate all the components into the OptiSystem layout. Next, factors like fibre length, pump power, and input signal levels are systematically varied. Tables and graphs are used to display the results and show how important factors relate to one another. This method makes it possible to determine the best EDFA configurations, which advances the creation of high-performance, energy-efficient amplifiers for use in submarine networks, DWDM systems, and other cutting-edge optical applications [11] and [12].

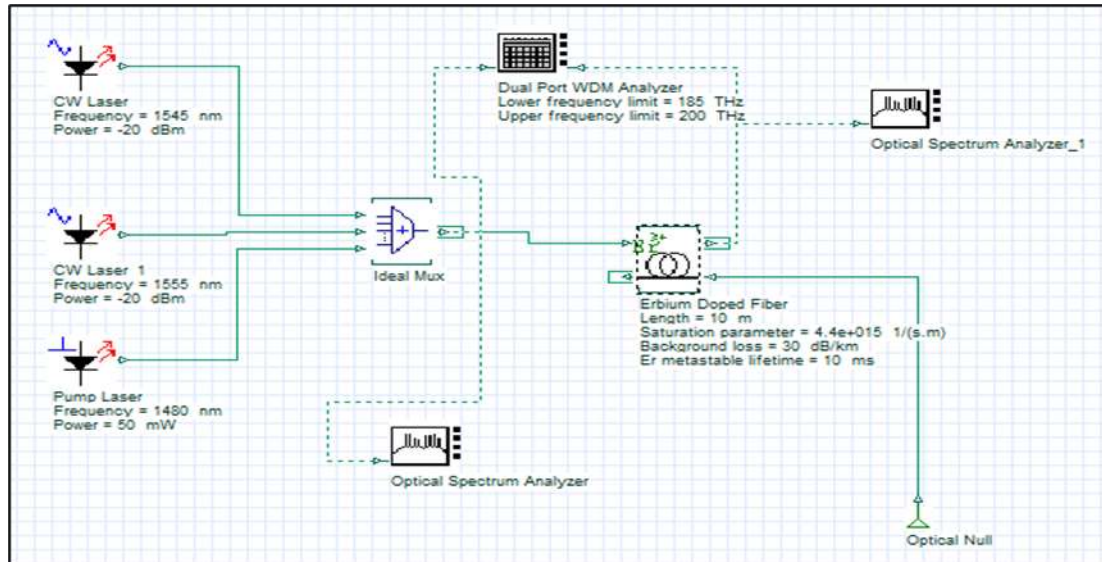


**Fig. 1** Simulation of EDFA in Optisystem

### 3. Result and Discussion

The results of the simulation and analysis of the Erbium-Doped Fibre Amplifier (EDFA) model using OptiSystem software are shown Fig. 1. This study's main goals were to determine the best configurations for realistic optical communication systems and to look at how fibre length affects the gain, efficiency, and noise characteristics of EDFAs. The study methodically assessed how many parameters, including pump power, input signal power, and fibre length, affect the amplifier's overall performance using numerical simulations.

Key performance parameters, such as gain, noise figure, and output power, are examined in relation to the simulation findings spanning the S-band, C-band, and L-band wavelength bands. The Wavelength Division Multiplexer (WDM) analyser and the Optical Spectrum Analyser (OSA) both produce graphical outputs that shed light on how the amplifier behaves under various operating circumstances. The results show the trade-offs between noise reduction and signal amplification, highlighting the nonlinear relationship between fibre length and gain. Additionally, the findings highlight how crucial it is to maximise efficiency while reducing ASE noise by optimising pump power and fibre length.

In addition to comparing the simulation results with theoretical predictions, this section offers a thorough analysis of the patterns and irregularities found in the data. By combining these results, the study provides helpful advice for creating EDFAs that are suited to the requirements of sophisticated optical networks such as Dense Wavelength Division Multiplexing (DWDM) systems. The study provided here emphasises how important fibre length and other crucial factors are to maximising EDFA performance for long-distance and high-speed communication.

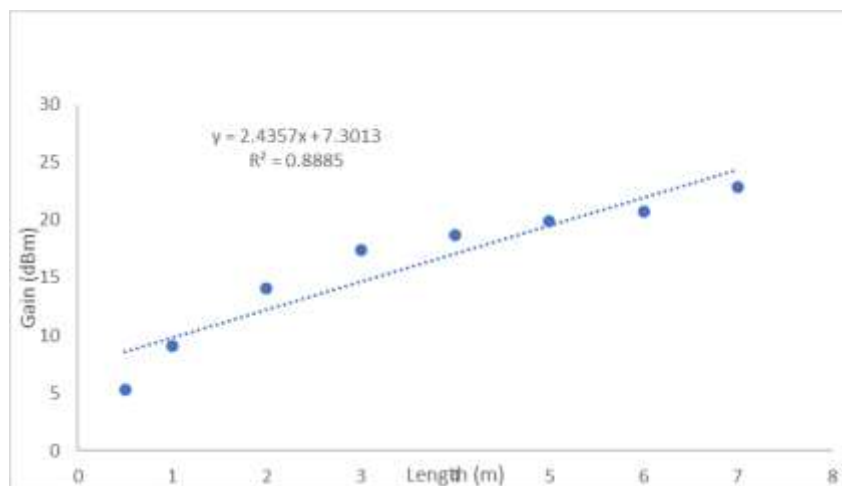


**Fig. 2** Graph of Characterization

Fig. 2 illustrates how length and gain are related, displaying a positive linear trend in which gain rises with length. Starting with an intercept of 7.3013, the trendline equation ( $y = 2.4357x + 7.3013$ ) shows that the gain increases by about 2.44 for every unit increase in length. Although there are slight variations at longer lengths, the ( $R^2$ ) value of 0.8885 indicates a good correlation between length and gain. This graph provides a forecast tool for system performance and accurately depicts the behaviour of the system, showing steady gains with length.

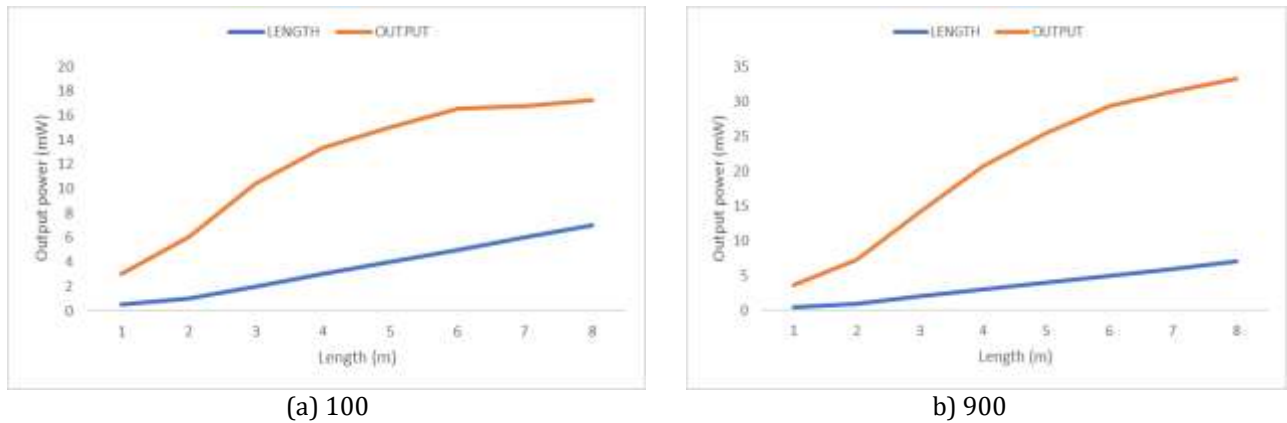


**Fig. 3** (a) Graph output power vs length (100) pump laser; (b) Graph output power vs length (900) pump laser

Both depicted lines in the Fig. 3(a) shows a comparatively linear relationship between length (x-axis, measured in meters) and output power (y-axis, measured in milliwatts). As the length increases, the output power of the blue line with the label "LENGTH" steadily rises, showing a straight proportionality between the two factors. But after five meters, the orange "OUTPUT" line displays a more gradual slope after a faster initial climb. As length rises, the curve appears to flatten out a little, indicating decreasing efficiency. This behaviour might indicate a situation in which length increases output power but the system eventually reaches a point where length decreases output efficiency.

The relationship between length and output power is likewise depicted in the Fig. 3(b), albeit the output power growth rate is far faster in this case. The slopes of both lines are steeper than in the first graph. A very efficient system that converts length increases into a significantly larger gain in output power is indicated by the orange "OUTPUT" line, which rises quickly from 5 mW at 1 meter to over 35 mW at 8 meters. The curve stays on a steep trajectory the entire time, and the diminishing returns impact is much less noticeable than in the first graph. This might be an example of a system with improved technology or design that optimises the gearbox or conversion of length into output power.

It is clear from comparing the two graphs that the system shown in the second one is more effective. The output power in the second graph is continuously greater and grows at a significantly faster rate than in the first graph for the same length range (1–8 meters). For instance, the output power in the first graph is about 18 mW at 8 meters, whereas in the second graph, it surpasses 35 mW. A better design or mechanism that maximises energy transfer or utilisation is indicated by the second graph's orange line's steeper slope, which emphasises the system's increased responsiveness to length variations. All things considered; the second graph shows a system that is substantially more efficient since it can produce a higher output power under the same input conditions.

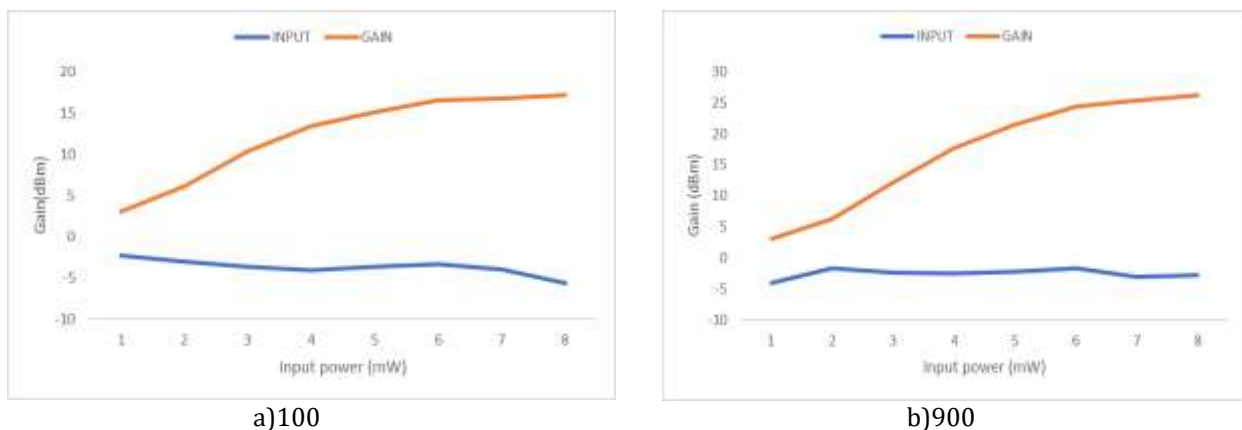
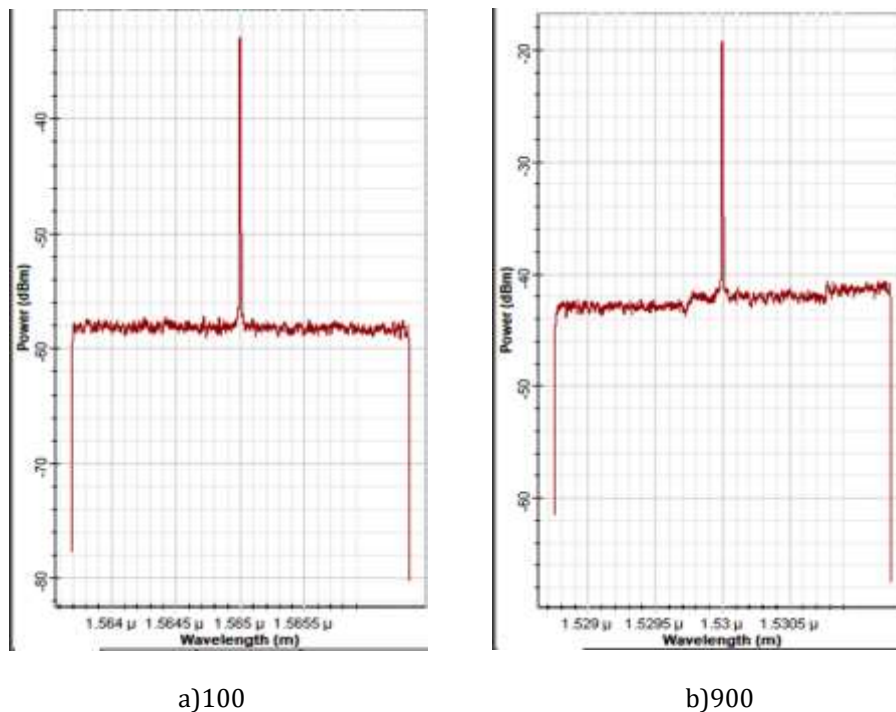


**Fig. 4** (a) Graph gain vs input power (100) pump laser; (b) Graph gain vs input power (900) pump laser

The link between input power (x-axis, in mW) and gain (y-axis, in dBm) is depicted in Fig. 4(a). Over the range of 1 to 8 mW, the input power, represented by the blue line, stays nearly constant between -5 dBm and 0 dBm. This suggests that there are only slight fluctuations in the input power, which stays comparatively constant. Conversely, the orange line, which represents gain, has a growing trend, peaking at around 18 dBm at 6 mW after beginning at about 5 dBm at 1 mW. The gain curve flattens down beyond 6 mW, suggesting that as input power rises further, gain efficiency decreases. This implies that while the system is effective at lower input levels, it reaches saturation at which more input power results in less noticeable gains.

The link between input power and gain is also depicted in Fig. 4(b), albeit the performance is substantially better. Over the range of 1 to 8 mW, the input power blue line is comparatively constant, varying only slightly around the 0 dBm level. Compared to the first graph, the orange gain line exhibits a substantially steeper increase, rising from 5 dBm at 1 mW to about 30 dBm at 8 mW. The gain curve does not significantly flatten out like it did in the first graph, suggesting that even at greater input levels, the system is still able to convert input power into gain effectively. This behaviour points to a system that is well-optimized, has low losses, and can handle larger input power.

Fig. 4(b) is substantially more efficient than the first when the two graphs are compared. In contrast to the first system's 18 dBm peak, the second system achieves a substantially greater gain of 30 dBm over the same input power range of 1 to 8 mW. Furthermore, beyond 6 mW, the first system's gain curve plateaus, indicating a drop in efficiency, while the second system's gain increases steadily and sharply over the range. This shows that the second system is more efficient at turning input power into gain and has superior power-handling capabilities. Although the input appears to be constant based on the stable input power curve in both plots, the second system performs noticeably better in terms of gain optimisation. Overall, the second system performs better than the first in terms of sustained efficiency and maximum gain.



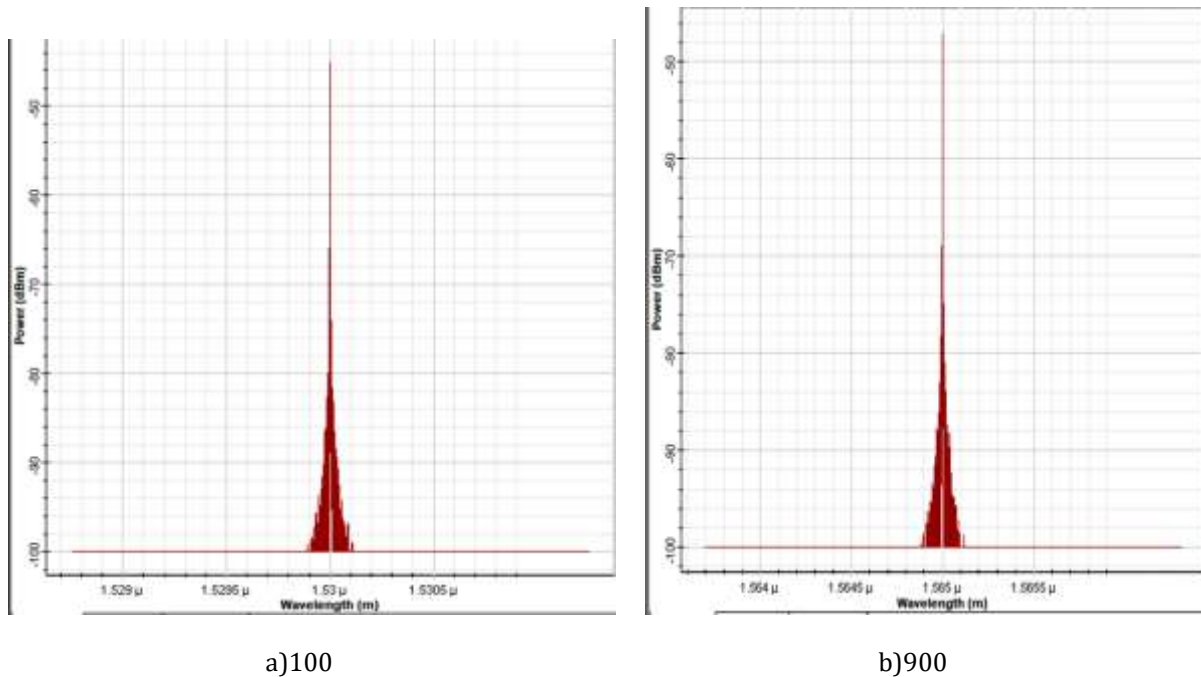
**Fig. 5** (a) Gain spectrum for output signal (100) pump laser; (b) Gain spectrum for output signal (900) pump laser

Fig. 5(a) shows a power spectrum with a maximum power level of roughly -40 dBm and a peak centred at about 1.565  $\mu\text{m}$ . Excellent spectral purity and a well-optimized system for minimising dispersion are reflected in the peak's extreme narrowness, which shows that the power output is highly concentrated at this particular wavelength. At about -60 dBm, the baseline power outside the peak is rather steady, indicating low noise throughout the whole wavelength range. For applications such as optical communications and high-precision laser systems, the system's ability to efficiently suppress power at non-target wavelengths is confirmed by the severe drop-off on either side of the peak. Fig. 5(a) illustrates a precision-engineered system where wavelength targeting and low noise are top concerns.

A power spectrum is also displayed in Fig. 5(b) with its peak centred at roughly 1.53  $\mu\text{m}$ . At -20 dBm, the peak power is 20 dBm higher than the peak power in the first graph, indicating a considerable increase. The peak's sharpness is similar to that of the first graph, suggesting good spectral focus and little power spreading outside of the core wavelength. This graph's baseline noise level is little higher, staying at about -50 dBm

throughout the spectrum. Applications that require extremely low-noise conditions may be impacted by the system's modest increase in baseline noise, even if it provides more power. However, the notable increase in peak power indicates that this system is more appropriate for high-output situations where maximising power is more crucial than preserving the lowest noise levels.

In terms of power output, the Fig. 5(b) is more efficient than Fig. 5(a). It is better suited for applications requiring high-energy output since its peak power of -20 dBm is far higher than the first system's -40 dBm peak power. Strong wavelength targeting is also demonstrated by the second graph's sharper, more distinct peak, which maintains a high degree of spectral purity in spite of the higher baseline noise (-50 dBm as opposed to -60 dBm in the first system). However, because it keeps the baseline noise level lower across the spectrum, the first method performs exceptionally well in terms of noise reduction. Because of this, the first system is perfect for settings that demand high signal-to-noise ratios or applications where a clear signal with less noise is crucial.



**Fig. 6** (a) Gain spectrum for input signal (100) pump laser; (b) Gain spectrum for input signal (900) pump laser

A power spectrum is displayed in Fig. 6(a), with the peak centred at roughly 1.53  $\mu\text{m}$ . The peak's maximum power, which is approximately -50 dBm, indicates a signal that is relatively powerful. The peak has a minimal full width at half maximum (FWHM) and is extremely thin and sharply defined. This exhibits exceptional spectral purity, which lowers interference with nearby wavelengths because the majority of the signal power is contained inside a single wavelength. A very low-noise environment, which is necessary for systems with high signal-to-noise ratios (SNR), is reflected in the baseline noise level of about -100 dBm. Fig. 6(a) represents a system that is optimised for precision and low dispersion, which makes it appropriate for tasks where accuracy is crucial, such as narrowband optical systems or laser applications. However, the comparatively low peak power (-50 dBm) indicates that stability and low interference are its primary goals rather than high-energy output scenarios.

With a peak centred at 1.565  $\mu\text{m}$ , Fig. 6(b) displays a power spectrum. Its maximum power is roughly -40 dBm, 10 dBm higher than the first graph's. The system maintains great spectrum efficiency and accurate wavelength targeting, as seen by this peak's narrowness and correspondingly low FWHM. Similar to the first graph, the baseline noise level stays at about -100 dBm, showing that this system likewise functions in a low-noise environment. The increased peak power, however, shows that this system can produce more energy while preserving noise reduction and spectral focus. These features make it appropriate for uses such as optical amplifiers, wavelength division multiplexing (WDM), and other high-performance communication systems that demand both accuracy and higher power levels.

In general, Fig. 6(b) is more efficient than the first. It can supply more energy at its core wavelength since its peak power of -40 dBm is far higher than the first system's -50 dBm. Both systems have tight, distinct peaks and great spectral focus. Additionally, their baseline noise levels at -100 dBm are the same, indicating equivalent noise suppression performance. But because of its larger power output, the second technology is more adaptable to applications that need more precise energy transfer. On the other hand, applications where

minimal power suffices and minimising interference is crucial are better suited for the first system, which has the same noise suppression but a somewhat lower power.

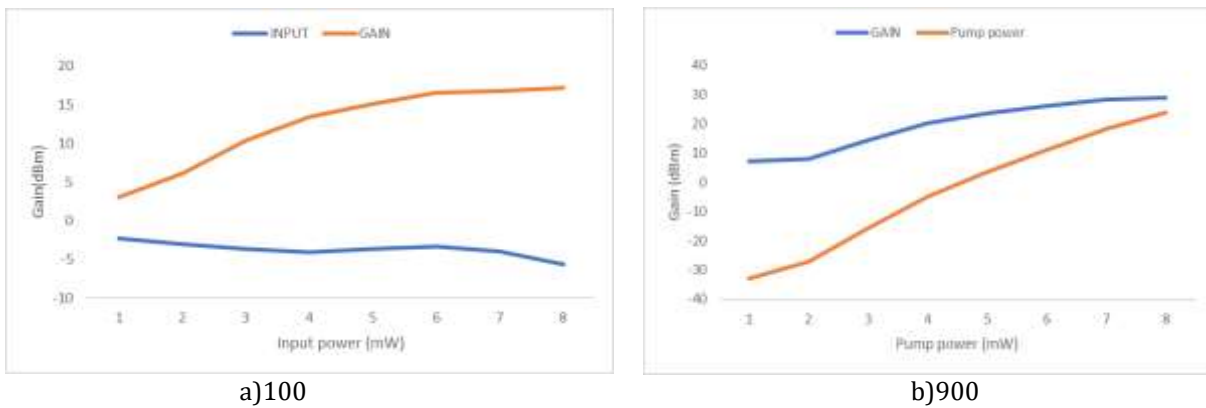


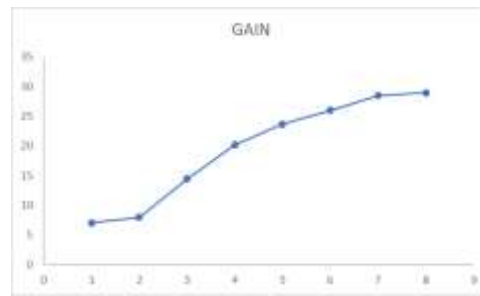
**Fig. 7** (a) Graph Pump power vs Gain (100) pump laser; (b)Graph Pump power vs Gain (900) pump laser

The link between input power (x-axis, in mW) and gain (y-axis, in dBm) is depicted in Fig. 7(a). The input power is represented by the blue line, which begins at about -5 dBm and progressively decreases as the input power rises from 1 mW to 8 mW. This decrease implies that the system is using input power less effectively at higher power levels yet is consuming more of it as power increases. The gain is shown by the orange line, which starts at about 5 dBm at 1 mW of input power and increases gradually until it peaks at about 20 dBm at 8 mW. Nevertheless, the gain curve begins to somewhat flatten at 6 mW of input power, showing declining returns. This flattening implies that when input power increases more, the system's capacity to transform more input power into gain diminishes. Although this system has a saturation point where further increases in input power result in negligible extra gain, it looks to be somewhat efficient.

The relationship between gain (y-axis, in dBm) and pump power (x-axis, in mW) is displayed in Fig. 7(b). Gain is shown by the blue line, which begins at around 10 dBm at 1 mW of pump power and increases gradually to about 35 dBm at 8 mW. In contrast to the previous graph, the gain curve shows no discernible flattening and instead continues on an increasing trend over the whole range. This suggests a very effective mechanism that reliably turns pump power into gain. The system's pump power appears to scale well with the gain, as seen by the orange line, which represents pump power. It begins at about -30 dBm at 1 mW and climbs dramatically to about 10 dBm at 8 mW. This system's excellent performance is highlighted by the proportional and linear relationship between pump power and gain, which exhibits few symptoms of saturation or inefficiency.

Fig. 7(b) is obviously more efficient than the first when the two are compared. The gain reaches a much higher value of 35 dBm in the second graph, whereas it peaks at 20 dBm in the first. Furthermore, the first system's efficiency is limited at higher power levels due to diminishing returns, as shown by the gain curve flattening at 6 mW of input power. Fig. 7(b), on the other hand, shows a steady and linear increase in gain without any indications of saturation, suggesting continued efficiency over the power range.





c) L band

**Fig. 8** (a) Gain for S band; b) Gain for C band c) Gain for L band

Fig. 8(a) for S band shows how GAIN changes in response to an independent variable, most likely pump power or input power. Starting at roughly 5 dBm at the first data point and progressively rising to about 25 dBm at the last, the trend demonstrates a steady and positive increase in gain. From points 1 through 4, the curve exhibits an initially sharper increase, suggesting a significant reaction or efficiency in gain improvement in this region. The slope gets more gradual after point 4, suggesting that gains reduce as the variable rises. Higher numbers cause the curve to slightly flatten, which indicates that the system is getting close to its saturation point or maximum efficiency.

With values steadily rising from the first to the last data point, Fig. 8(b) for C band illustrates how GAIN varies over an independent variable. The gain initially shows a quick improvement, beginning at around 5 dBm at point 1 and increasing sharply to about 25 dBm by point 4. A slower pace of increase is shown by the curve's minor flattening after point 4. The gain exhibits plateau-like behaviour between points 4 and 6, which could indicate a phase of transition in system efficiency or diminishing returns. The gain starts a consistent increasing trend at point 6 and reaches about 30 dBm at point 8.

With a distinct pattern of rising gain over the measured range, Fig. 8(c) for L band illustrates the evolution of GAIN as a function of an independent variable. The gain first begins at point 1 at about 10 dBm and then gradually increases to point 2. The gain increases more sharply from point 2 to point 4, reaching about 25 dBm. This suggests that the gain improved significantly throughout this time. As the independent variable rises past point 4, the curve flattens down and shows a slower rate of increase, indicating diminishing returns. From point 6 onward, the gain reaches a more stable range, plateauing slightly near 30 dBm by point 8. When comparing the three Fig. 8, Fig. 8(b) for C band emerges as the most efficient. It obtains the greatest gain (30) with a steady growth rate, showing stable performance and long-term dependability. Fig. 8(c) for L band, despite obtaining the same peak gain as Fig. 8(b) for Graph C band, is slightly less efficient due to the plateau shown in the later intervals, indicating a reduction in marginal returns over time. Fig. 8(a) for S band is the least efficient model since it lags behind in both total gain (25) and growth rate.

#### 4. Conclusion and Recommendation

In order to determine the gain and efficiency of Erbium-Doped Fibre Amplifiers (EDFAs), which are crucial for contemporary optical communication systems, this study emphasises the crucial significance that fibre length plays. Fibre length has a significant impact on the interaction between pump light and erbium ions, according to systematic simulations conducted with OptiSystem. Shorter fibres result in insufficient amplification, while longer fibres cause amplified spontaneous emission (ASE) noise and efficiency losses. The study provides important information for creating high-performance EDFAs by determining the ideal fibre length that optimises gain and efficiency while reducing noise. These results are especially pertinent to applications like long-distance optical links, submarine communication networks, and Dense Wavelength Division Multiplexing (DWDM), where dependable and effective signal amplification is essential to satisfying the expanding demand for high-speed data transmission worldwide.

To further improve EDFA performance, future studies should examine the combined effects of other crucial characteristics, such as pump wavelength, core geometry, and erbium ion distribution, in addition to fibre length. Investigating hybrid optical amplification systems that combine EDFAs with semiconductor or Raman amplifiers may increase overall efficiency and wavelength coverage. To support global sustainability goals, practical implementations should give priority to energy-efficient designs that are suited to particular applications, such as space-based, undersea, or terrestrial communication systems. Furthermore, funding cutting-edge simulation programs, experimental configurations, and industry partnerships will hasten the creation of next-generation optical amplifiers, guaranteeing their scalability, affordability, and capacity to satisfy the growing needs of contemporary optical networks.

## Acknowledgement

The author would like to thank the Faculty of Applied Sciences and Technology Malaysia for its support. The cooperation is much supported.

## Conflict of Interest

Authors declare that there is no conflict of interests regarding the publication of the paper.

## Author Contribution

*The authors confirm contribution to the paper as follows: **study conception and writing:** Naquiuddin Razali; **guidance and made corrections:** Noor Azura Awang. All authors reviewed the results and approved the final version of the manuscript.*

## References

- [1] M.-S. Alouini, X., Liu, & Z., Zhu. (2020). Optical communications and networks. *IEEE Communications Magazine*, 58(2), 12.
- [2] Reddy, V. V., Rajalakshmi, B., Thethi, H. P., Kumar, V., Kumar, A., & Alkhafaji, M. A. (2023). Optical communication systems for ultra-high-speed data transmission. In 2018 5th IEEE Uttar Pradesh Section International Conference on Electrical, Electronics and Computer Engineering (UPCON) (pp. 1569–1574).
- [3] Giles, C. R., Desurvire, E., Zyskind, J. L., & Simpson, J. R. (1990). Erbium-doped fiber amplifiers for high-speed fiber-optic communication systems. In *SPIE Proceedings* (Vol. 1171, p. 318).
- [4] Malakzadeh, A., Pashaie, R., & Mansoursamaei, M. (2020). Gain and noise figure performance of an EDFA pumped at 980 nm or 1480 nm for DOFSs. *Optical and Quantum Electronics*, 52(2).
- [5] Desurvire, E. (1990). Erbium-doped fiber amplifiers for optical fiber communications. In *Optical Amplifiers and Their Applications* (pp. MB1–MB1).
- [6] Otani, T., Goto, K., Kawazawa, T., Abe, H., & Tanaka, M. (1997). Effect of span loss increase on the optically amplified communication system. *Journal of Lightwave Technology*, 15(5), 737–742.
- [7] Fan, W., et al. (2021). Demonstration of optical gain at 1550 nm in an Er<sup>3+</sup>-Yb<sup>3+</sup> co-doped phosphate planar waveguide under commercial and convenient LED pumping. *Optics Express*, 29(8), 11372–11372
- [8] Z. Zhang et al. (2018). "21 spatial mode erbium-doped fiber amplifier for mode division multiplexing transmission," *Optics Letters*, vol. 43, no. 7, pp. 1550–1550, Mar. 2018.
- [9] Bouzid, B. (2011, April). Theoretical analysis of erbium doped fiber amplifier (pp. 1–5).
- [10] Pal, M., et al. (2007). Investigation of the optical gain and noise figure for multi-channel amplification in EDFA under optimized pump condition. *Optics Communications*, 273(2), 407–412.
- [11] Singh, K. (2017). Performance evaluation of hybrid optical amplifier in fiber optical communication system.
- [12] Zyskind, J. L. (1992). Erbium-doped fiber amplifiers. In *Proceedings of SPIE, the International Society for Optical Engineering* (Vol. 1581, pp. 14–23).